Unveiling the influence of heating temperature on biofilm formation in shower hoses through multi-omics

Yao, Mingchen; Ren, Anran; Yang, Xiangyu; Chen, Lihua; Wang, Xun; van der Meer, Walter; van Loosdrecht, Mark C.M.; Liu, Gang; Pabst, Martin

DOI
10.1016/j.watres.2024.122704

Publication date
2024

Document Version
Final published version

Published in
Water Research

Citation (APA)
Yao, M., Ren, A., Yang, X., Chen, L., Wang, X., van der Meer, W., van Loosdrecht, M. C. M., Liu, G., & Pabst, M. (2024). Unveiling the influence of heating temperature on biofilm formation in shower hoses through multi-omics. *Water Research*, *268*, Article 122704. https://doi.org/10.1016/j.watres.2024.122704

Water Research 268 (2025) 122704

Contents lists available at ScienceDirect

Water Research

journal homepage: www.elsevier.com/locate/watres

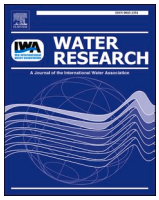

Unveiling the influence of heating temperature on biofilm formation in shower hoses through multi-omics

Mingchen Yao [a,b,c,1], Anran Ren [a,b,1], Xiangyu Yang [d,e], Lihua Chen [c], Xun Wang [f], Walter van der Meer [g], Mark C.M. van Loosdrecht [f], Gang Liu [a,b,c,*], Martin Pabst [f]

[a] Key Laboratory of Drinking Water Science and Technology, Research Centre for Eco-Environmental Sciences, Chinese Academy of Sciences, Beijing, 100085, China
[b] University of Chinese Academy of Sciences, Beijing, China
[c] Sanitary engineering, Department of Water management, Faculty of Civil Engineering and Geosciences, Delft University of Technology, P.O. Box 5048, 2600 GA Delft, the Netherlands
[d] Shandong Provincial Key Laboratory of Marine Environment and Geological Engineering (MEGE), College of Environmental Science and Engineering, Ocean University of China, 238 Songling Road, Qingdao 266100, PR China
[e] Key Laboratory of Marine Environment and Ecology, Ministry of Education, College of Environmental Science and Engineering, Ocean University of China, Qingdao 266100, PR China
[f] Department of Biotechnology, Delft University of Technology, Delft, the Netherlands
[g] Membrane Science and Technology, Faculty of Science and Technology, Twente University, the Netherlands

ARTICLE INFO

Keywords:
Shower hose biofilm
Metagenomics
Metaproteomics
Biosafety
Heating temperature

ABSTRACT

Shower systems provide unique environments that are conducive to biofilm formation and the proliferation of pathogens. The water heating temperature is a delicate decision that can impact microbial growth, balancing safety and energy consumption. This study investigated the impact of different heating temperatures (39 °C, 45 °C, 51 °C and 58 °C) on the shower hose biofilm (exposed to a final water temperature of 39 °C) using controlled full-scale shower setups. Whole metagenome sequencing and metaproteomics were employed to unveil the microbial composition and protein expression profiles. Overall, the genes and enzymes associated with disinfectant resistance and biofilm formation appeared largely unaffected. However, metagenomic analysis revealed a sharp decline in the number of total (86,371 to 34,550) and unique genes (32,279 to 137) with the increase in hot water temperature, indicating a significant reduction of overall microbial complexity. None of the unique proteins were detected in the proteomics experiments, suggesting smaller variation among biofilms on the proteome level compared to genomic data. Furthermore, out of 43 pathogens detected by metagenomics, only 5 could actually be detected by metaproteomics. Most interestingly, our study indicates that 45 °C heating temperature may represent an optimal balance. It minimizes active biomass (ATP) and reduces the presence of pathogens while saving heating energy. Our study offered new insights into the impact of heating temperature on shower hose biofilm formation and proposed optimal parameters that ensure biosafety while conserving energy.

1. Introduction

Ensuring the biosafety of drinking water in modern societies is both critical and challenging (Edition, 2011; Ramírez-Castillo et al., 2015; Falkinham et al., 2015). Between 2000–2015, 17 waterborne diseases caused 7.15 million infections annually in the United States, incurring $3.3 billion in economic losses (Collier et al., 2021). The World Health Organization (WHO) reported that >505,000 deaths are attributed to waterborne pathogens each year (World Health Organization 2024). As the very front line directly facing customers, shower systems have been recognized as hotspots for the accumulation of (opportunistic) pathogens and infections (Feazel et al., 2009; Gebert et al., 2018; Proctor et al., 2018; Schoen and Ashbolt, 2011; Shen et al., 2022; Darelid et al., 2002). For example, the Legionnaires' outbreak in Stavanger, Norway was contracted from municipal showers (Krovel et al., 2022). Shen et al. demonstrated recently that viable nontuberculous mycobacteria can be transferred from water to air during showering (Shen et al., 2022). Microorganisms in showers primarily exist in biofilms. Particularly, shower

* Corresponding author at: Chinese Academy of Science, Delft University of Technology.
E-mail addresses: gliu@rcees.ac.cn, g.liu-1@tudelft.nl (G. Liu).
[1] Mingchen Yao and Anran Ren contribute equally to this work.

https://doi.org/10.1016/j.watres.2024.122704
Received 20 August 2024; Received in revised form 19 October 2024; Accepted 25 October 2024
Available online 28 October 2024

hoses provide an ideal niche for biofilm formation, because of the warm temperatures, large surface/volume ratio, long stagnation (~ 23.8 h/day), low disinfectant residual and nutrient migration from flexible plastic materials (Proctor et al., 2018; Rhoads et al., 2016; Bucheli--Witschel et al., 2012; Proctor et al., 2016). Therefore, having a comprehensive understanding of shower hose biofilm formation is of utmost importance.

The advancement of DNA-based technologies has significantly advanced our understanding of shower hose biofilms. However, studies were only limited to the usage of 16S rRNA gene amplicon sequencing and/or quantitative polymerase chain reaction (q-PCR) (Proctor et al., 2018; Proctor et al., 2016; Cavallaro et al., 2023). These approaches have well-known primer-biasand do not provide functional information (Dai et al., 2020). These limitations can be overcome by the application of whole metagenome sequencing (metagenomics). However, only a few studies employed metagenomics to investigate shower hose biofilms (Soto-Giron et al., 2016). Furthermore, metagenomics alone does not provide critical information regarding active microbiota and the expression of metabolic pathways and enzymes. For example, (opportunistic) pathogens have been widely detected and reported in shower systems. The exposure risk assessment is challenging due to the inability to determine the pathogen's viability or presence at relevant levels. Recently, multi-omics approaches, combining metagenomics and metaproteomics have been employed in biological water treatment systems to unveil the active microbiome and core functions within these communities (Kleikamp et al., 2023; Tian and Wang, 2021). However, research on biofilms in shower hoses utilizing a multi-omics approach has not been conducted yet.

When it comes to shower systems, temperature is the most important factor to be considered because it can be adjusted to balance biosafety and energy conservation (Rhoads et al., 2015; Ji et al., 2017; Proctor et al., 2017). For biosafety, WHO, National Academy of Science, Engineering and Medicine (NASEM) and Centers for Disease Control and Prevention (CDC) recommend heating and storing water above 60 °C and 55 °C within recirculation loops (World Health Organization 2024; National Academies of Sciences E, Medicine 2020; Centers for Disease Control and Prevention 2024). The U.S. Department of Energy (DOE) recommends setting water heaters to 46–49 °C for energy efficiency (U.S. Department of Energy 2024). Higher temperatures could mitigate the risk of pathogen growth and influence microbiota in hot water plumbing (Darelid et al., 2002; Rhoads et al., 2015; Ji et al., 2017; Proctor et al., 2017). Regardless of the heated-up temperatures, the hot water has to be mixed with cold water for a usable and comfortable temperature (i.e., ~39 °C) for showering, which is the temperature of influent for shower hose biofilm. However, the critical question such as the influence of heated-up temperatures on shower hose biofilm remains unknown.

In this study, we investigated the influence of temperature settings on the shower hose biofilm, by using four controlled full-scale shower systems (water heater at 39, 45, 51 and 58 °C). Shower hose biofilm samples were collected to study the microbiome both in situ and in vitro. Most importantly, whole metagenome sequencing and metaproteomics were employed to understand the genomic composition and expressed functions at different heating temperatures. The results provide new insights into the impact of temperature on shower hose biofilms and help identify synergy between biosafety and energy conservation.

2. Materials and methods

2.1. Full-scale shower systems

The shower hoses were collected from four controlled full-scale shower systems. Each shower system was equipped with an instantaneous water heater and three parallel shower units. The hot and cold water pipes were made of nominal 1/2-inch polypropylene-random (PPR) pipes. The shower hoses were made of polyvinyl chloride (PVC) hoses (Submarine, China), with an inner diameter of 0.85 cm. Shower systems were fed with tap water from Changchun (Jilin province, China). The set temperatures of the four water heaters were 39, 45, 51 and 58 °C, respectively (Rhoads et al., 2015; Ji et al., 2017; Proctor et al., 2017). The shower units were flushed (simulated bath) every day and each flush controlled the outlet water to 39±1 °C for 8 min at 4.2 ± 0.4L/min. After three months of incubation, twelve shower hoses were collected for subsequent biofilm analysis.

2.2. Biofilm sampling

After the shower hose was removed, the exterior was immediately disinfected with chlorine and transferred to a clean bench for further treatment. The total length of the shower hose was 1.5 m. The hose was cut into three sections (length = 50 cm) with a pipe cutter. A 5 cm section was then cut off at one end of the three hoses and carefully cut into pieces, followed by storing them in sterile phosphate buffer solution (PBS, pH=7.2) for in situ characterization of the biofilm structure. To maximize biofilm sample collection, a biofilm sampler was invented, which consisted of a silicone plug with the same outer diameter as the inner diameter of the shower hose and a stainless-steel tube. The sampler was cleaned with ultrapure water and sterilized before use. The biofilm in the remaining three sections of shower hose (length = 45 cm) was pushed into a sterile centrifuge tube using the biofilm sampler. The biofilm sampler was then rinsed with PBS and the rinse solution was collected. The above steps were repeated three times to obtain a microbial suspension. The obtained suspensions were then used for further microbiological analysis. All samples were stored at 4 °C for further processing within 2 h.

2.3. Water quality analysis

Quadruplicate influent water samples were collected once a month during the growth phase. Free and total chlorine was measured on-site using a spectrophotometer (HACH DR300). The total organic carbon (TOC) concentration was determined by a TOC analyzer (Shimadzu, Japan). The concentrations of aluminum (Al), iron (Fe), manganese (Mn), cuprum (Cu) and zinc (Zn) were determined by inductively coupled plasma–mass spectrometry (Thermo Fisher Scientific, America). The concentrations of magnesium (Mg) and calcium (Ca) were measured using inductively coupled plasma optical emission spectroscopy (Shimadzu, Japan). The concentrations of chloride (Cl^-), sulfate (SO_4^{2-}) and nitrite (NO_3^-) ions were analyzed with ion chromatography (IC, Dionex, USA). The influent water quality parameters at each sampling time are presented in Table S1.

2.4. Adenosine triphosphate (ATP) and flow cytometry cell count

Total ATP concentrations were measured to determine the active biomass. ATP measurements were conducted using the GloMax® Navigator Microplate Luminometer (Promega, USA) and the Water-Glo™ reagent (Promega, USA) as described previously (Yao et al., 2023). Briefly, 800 μL of the obtained suspension was mixed with 200 μL of lysis reagent and incubated for 2 h at room temperature. Then 125 μL of each sample was added to a 96-well plate in triplicate and an equal volume of Water-Glo detection reagent was automatically added by the luminometer injector. Finally, luminescence was measured following manufacturer's instructions. The results in relative light units were converted into the ATP concentrations using the obtained standard curve.

Flow cytometry (FCM) combined with fluorescence staining has been selected to quantify total cell counts (TCC) in obtained suspensions (Hammes et al., 2008; Sousi et al., 2018). The FCM (Agilent NovoCyte 1040®, USA) is equipped with 20 mW laser with an emission wavelength of 488 nm. Green fluorescence was collected in the FL1 channel (530 ± 30 nm). Samples were stained with 10 μL/mL SYBRs Green I (1:100 dilution in DMSO; Invitrogen, USA) and incubated in the dark at room temperature for 20 min. Finally, they were measured in triplicate

with FCM at 66 μL/min flow rate. Data was collected and processed with the NovoExpress™ software.

2.5. Characterization of biofilm structure

The biofilm surface morphology was characterised by scanning electron microscopy (SEM; FEI Quattro S, USA). Briefly, the pieces of shower hoses were fixed at 4 °C with 2.5 % glutaraldehyde for 6 h and then dehydrated with a series of concentration gradients of ethanol (30 %, 50 %, 70 %, 80 %, 90 %, 95 % and 100 %) with 15 min per step. They were then displaced with isoamyl acetate 2 times (15 min per step) and finally dried at the critical point (Automegasamdri-938 C, USA). The dried samples were characterized with SEM after they were sputter-coated with gold (E1010, Hitachi, Japan) for 60 s.

Confocal laser scanning microscopy (CLSM; TCS SP8 CSU, Leica, Germany) was employed to determine the distribution of the extracellular polymeric substance (EPS) on shower hose biofilm in situ. As previously reported (Chen et al., 2007; Yang et al., 2022), the shower hose pieces were washed with PBS 3 times and soaked in 0.1mol/L $NaHCO_3$ solution ensuring the amino group remained unprotonated. Fluorescein isothiocyanate (FITC), concanavalin A (Con A, tetramethylrhodamine conjugate), calcofluor white (CW) and Nile Red (NR) solutions were then added in order to stain proteins, α-polysaccharide, β-polysaccharide and lipids, respectively. At the end of each staining process, samples were washed carefully 3 times with PBS. The specific staining and fluorescence excitation parameters are presented in Table S2.

To detect eDNA (B-form and d-form), another copy of the shower hose pieces was washed with PBS and incubated with rabbit monoclonal antibody raised against Z-DNA[Z22] (Absolute Antibodies, Ab00783–23.0) (5 μg) and murine monoclonal antibody raised against B-DNA[3519] (Abcam, ab27156) (5 μg) in 1 mL of PBS that contained 5 % (w/v) BSA for 2 h Afterwards, samples were washed with PBS and stained with 1:200 dilution of goat anti-rabbit IgG conjugated to Alexa Fluor™ 594 (Invitrogen, A11001) and goat anti-mouse IgG conjugated to Alexa Fluor™ 488 (Invitrogen, A11037) in PBS that contained 5 % BSA for 1 h Finally, samples were washed with PBS (Buzzo et al., 2021). All staining procedures were carried out under dark conditions at room temperature. After dyeing, all samples were immediately imaged using a 63 × oil objective on CLSM. Images were collected and rendered by Imaris software (Oxford Instruments, UK).

2.6. Metagenomic analysis

2.6.1. DNA extraction, library construction and sequencing

The obtained suspensions were filtered through 0.2 μm polycarbonate membrane filters (Whatman, UK) and stored at -80 °C before DNA and protein extraction. Due to limitations in sample volume, parallel samples were combined for subsequent metagenomic and metaproteomic assays. Total genomic DNA was extracted using the E.Z.N.A.® Soil DNA Kit (Omega Bio-tek, Norcross, GA, U.S.) following manufacturer's instructions. The concentration and purity of extracted DNA were measured by TBS-380 (Thermo Fisher Scientific, USA) and NanoDrop2000 (Thermo Fisher Scientific, USA), respectively. DNA quality was examined with 1 % agarose gel.

DNA was fragmented by Covaris M220 (Gene Company Limited, China) with an average size of about 400 bp for library construction. Paired-end library was constructed via NEXTFLEX Rapid DNA-Seq (Bioo Scientific, Austin, TX, USA). Paired-end sequencing was conducted on Illumina Novaseq 6000 (Illumina Inc., San Diego, CA, USA) at Majorbio Bio-Pharm Technology Co., Ltd. (Shanghai, China). The sequencing data have been deposited in the NCBI Sequence Read Archive (SRA) under the accession number PRJNA1056656.

2.6.2. Sequence quality control and genome assembly

The generated Illumina reads were trimmed to remove adaptors and low-quality reads (length<50 bp or with a quality value <20 or having N bases) using fastp v0.20.0 (Chen et al., 2018). The reads were further assembled by MEGAHIT v1.1.2 (Li et al., 2015) and contigs with a length ≥ 300 bp were retained for further analysis.

2.6.3. Gene prediction, taxonomy, and functional annotation

Prodigal v2.6.3 (Hyatt et al., 2010) was used to identify open reading frames (ORFs) from the assembled contigs. The predicted ORFs with length ≥ 100 bp were retrieved and translated into amino acid sequences. All sequences with a 90 % sequence identity (90 % coverage) were clustered to obtain a non-redundant gene set using CD-HIT v4.6.1 (Fu et al., 2012). High-quality reads from each sample were mapped back to the non-redundant gene set using a 95 % identity threshold and TPM (Transcripts Per Million) values were calculated using the SOAPaligner v2.21 (Li et al., 2008). Representative genes were aligned to NCBI nr database using Diamond sequence aligner v0.8.35 (Buchfink et al., 2015) for taxonomic annotations. The human (opportunistic) pathogens (OPs) were identified based on the list of human pathogen species published by Mark Woolhouse et al. (Woolhouse et al., 2007). KOs and annotation of virulent factors was performed by Diamond v0.8.35 (Buchfink et al., 2015) with the KEGG database (Kanehisa et al., 2016) or the VFDB database (Liu et al., 2022), respectively. The blast e-value cutoffs were set to $1e^{-5}$.

2.7. Metaproteomic analysis

2.7.1. Protein extraction and proteolytic digestion

A label-free quantitative proteomic approach was used to determine the protein compositions of biofilm samples. Proteins were extracted from biofilm samples using the Tris-phenol protocol described previously (Keiblinger et al., 2012). A more detailed description of the procedure is provided in Text S1. The extracted proteins were quantified and quality checked using Bicinchoninic acid (BCA) Protein Assay Kit (Pierce, Thermo Fisher Scientific, USA), and sodium dodecyl sulfate-polyacrylamide gel electrophoresis (SDS-PAGE).

Approx. 100 μg of protein were further reduced with 100 mM Triethylammonium bicarbonate buffer (TEAB) and 10 mM tris-(2-carboxyethyl)-phosphine (TCEP) for 60 min at 37 °C, followed by alkylation with 40 mM Iodoacetamide (IAM) for 40 min at room temperature in the dark. Pre-cooled acetone (acetone: sample v/v = 6:1) was added and incubated at -20 °C for 4 h to precipitate the protein and to remove salt. Finally, samples were digested with trypsin (1:50 trypsin-to-protein mass ratio) overnight at 37 °C and then dried in a vacuum concentrator.

2.7.2. Peptide pretreatment and LC-MS/MS analysis

The peptides were resuspended in 0.1 % trifluoroaceticacid (TFA), then desalted with an Oasis® HLB 96-well plate (Waters, USA) and speed vac dried. Peptide concentrations were measured using a peptide quantification kit (Cat.23275, Thermo Fisher Scientific, USA). The purified peptides were diluted to 0.1 μg/μL by loading buffer (2 % acetonitrile and 0.1 % formic acid in HPLC-grade water) and analyzed by an EASY nano-LC 1000 system (Thermo Fisher Scientific, USA) coupled to a timsTOF Pro 2 mass spectrometer (Bruker, Germany) in a shotgun proteomic approach, present at Majorbio Co. Ltd. (Shanghai, China). Details are provided in Text S2. The mass spectrometric raw data have been deposited in the iProX database, with the project reference code PXD048122.

2.7.3. Database searching of shotgun proteomic data

The mass spectrometric raw data were searched and processed with the MaxQuant v2.0.3.1 (Cox and Mann, 2008) software against the non-redundant metagenomic-constructed database. The enzyme specificity was set to trypsin. Carbamidomethylation of cysteines was set as a fixed modification, while oxidation of methionines and protein N-terminal acetylation as variable modifications. Up to two missed cleavages per peptide were tolerated. The minimum length of peptide sequence

was 7 amino acids. A reversed sequence database was employed to maintain the false discovery rate (FDR) of peptide-spectrum matches below 1 %. At least one unique peptide identification was required to support the identification of a protein. Protein abundance was quantified based on normalized spectral protein intensity, as described previously (Luber et al., 2010; Wiśniewski et al., 2012). The relative abundance was obtained by normalization within each sample. Taxonomic and functional annotations of database-matched peptide sequences were based on the classifications obtained for the ORFs from the metagenomic reference sequence database, as described above.

2.8. Statistics

The alpha diversity was calculated using the Observed, Simpson's evenness and Shannon diversity indices. The pairwise Jaccard distances for the inter-sample microbial community composition and KO functional profile, were calculated in R (R Core Team, 2013; Allaire, 2012) via the phyloseq package (McMurdie and Holmes, 2013). Statistically significant differences between groups were evaluated by the Wilcoxon rank sum test using the rstatix package (Kassambara, 2019). Furthermore, the relative expression activity (REA) index was used to assess the relative activity level of a given microorganism, gene and KO. The normalized REA was calculated as:

$$REA = \frac{Relative\ abundance/percentage\ in\ protein\ dataset}{Relative\ abundance/percentage\ in\ DNA\ dataset}$$

3. Results

3.1. Quantitative and structural properties of shower hose biofilm

The biofilm formed on shower hoses ranged 0.04–0.11 ng ATP/cm^2 and 2.8–4.5 × 10^5 cells/cm^2. According to the SEM images, the biofilm was scattered and unevenly distributed on the hose wall, which can be classified as two morphologies of flat films (Fig. 1A) and mound-shaped microcolonies (Fig. 1D). As shown in Fig. 1(B and C), the film-like biofilm was covered by dispersed β-polysaccharide and lipid conjugates that could have assembled into coating-like structures to withstand environmental fluctuations. The eDNA existed as a coral reef-like structure, where the content of B-DNA was much higher than that of Z-DNA (>130-folds). Otherwise, the EPS of mound-shaped biofilm was mostly comprised of α-polysaccharides and proteins, with the proteins aggregated and nested in the core and α-polysaccharides evenly spread throughout the microcolonies (Fig. 1E). The eDNA exhibited clustered and patchy distribution, while the content of Z-DNA sharply increased (B-DNA/Z-DNA=14.8 vs. 138). Intriguingly, Z-DNA was mostly distributed inside the microcolony and surrounded by B-DNA, suggesting that the transition from B-DNA to Z-DNA might be initiated from the inside of the biofilm (Fig. 1F).

3.2. Microbial community structure and composition

In total, 453.79 million raw reads were obtained by shotgun metagenomic sequencing, which was further processed to construct a non-redundant gene set including 91,861 genes. For metaproteomic analyses, a total of 3805 proteins could be retrieved from 29,719 distinct peptide sequences identified from 85,309 peptide-spectrum matches. The sequencing and processing of metagenomes and metaproteomes data is summarized in Table S3.

The number of taxa obtained by metagenomics (MG) was significantly higher than those obtained by metaproteomics (MP) at all taxonomic levels (Fig. 2A and Table S4). This is reasonable, because MP does not include any amplification steps and therefore measures the active microbiota and the abundant taxonomies, whereas MG describes the entire genetic material including free DNA, active, dead and dormant microorganisms. Compared to MG, MP revealed significantly higher evenness ($P < 0.01$), but similar Shannon index (Fig. 2B, S1 and Table S4). In addition, violin plots showed that the pairwise Jaccard distances between the biofilm communities obtained by MG and MP were significantly higher than those estimated within each category (i.e., MG or MP). It indicated that the identified abundant and active microbial community of the biofilm was significantly different from that of the total genetic potential of the community (Fig. 2C).

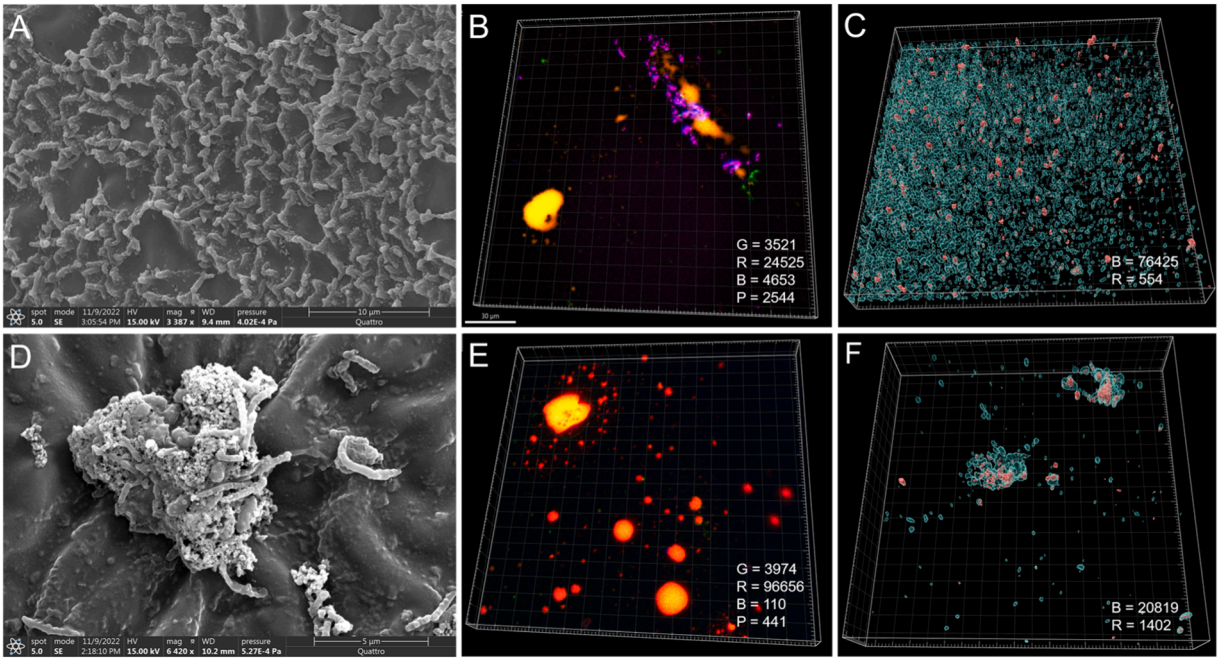

Fig. 1. The morphology and microstructure of biofilm. *A) and D) are scanning electron microscopy images of different biofilm morphologies; B) and E) are confocal laser scanning microscopy multichannel 3D images of biofilm EPS components, green (G) = protein, red (R) = α-polysaccharide, blue (B) = β-polysaccharide, purple (P) = lipid; C) and F) are confocal laser scanning microscopy multichannel 3D images of extracellular DNA, blue (B) = B-form DNA, red (R) = Z-form DNA. A-C are images of film-like biofilm, and d-F are images of mound-shaped biofilm.*

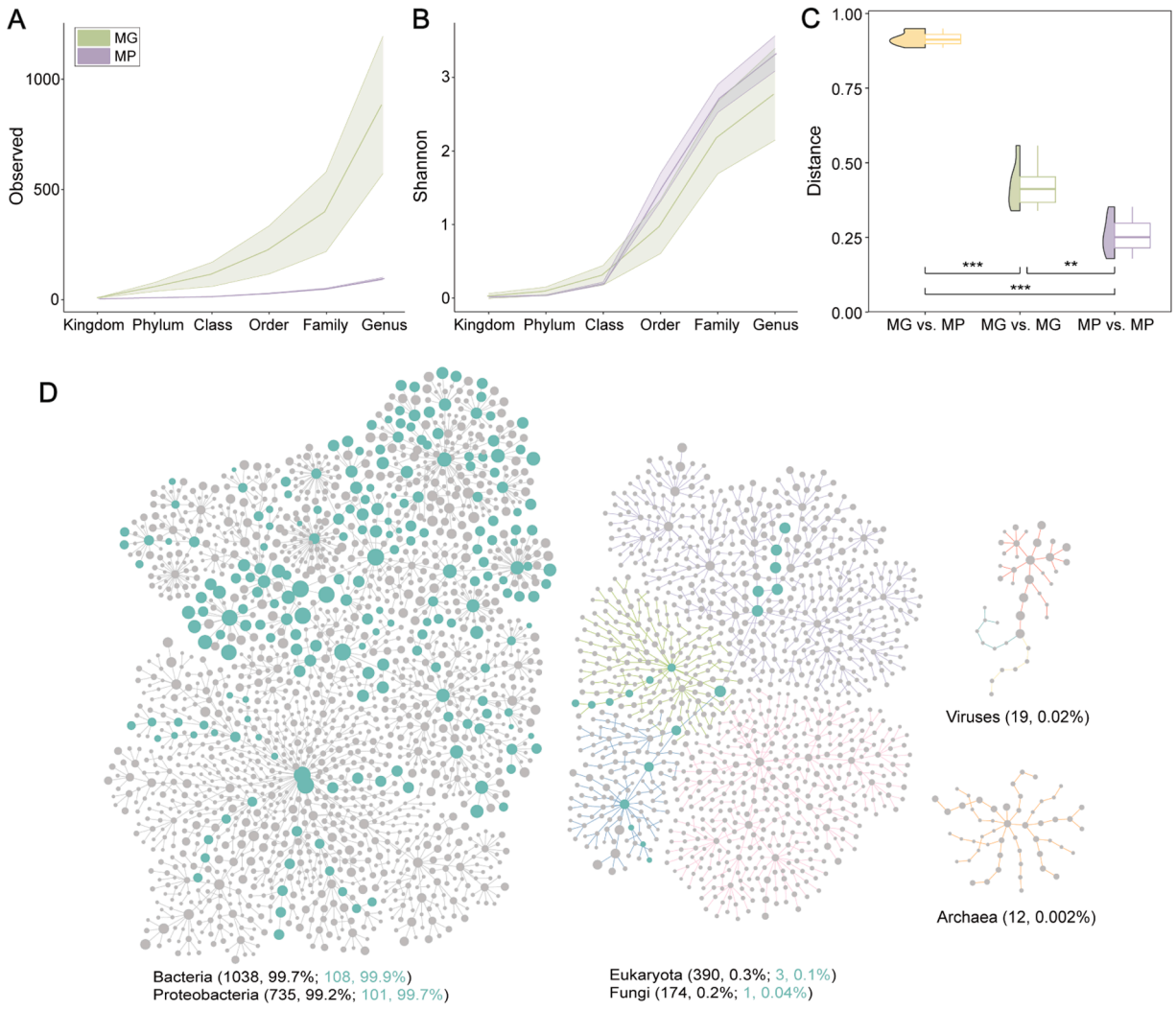

Fig. 2. The microbial community of hose biofilms revealed by metagenomics and metaproteomics. *Observed indices (A) and Shannon diversity (B) at all taxonomic levels revealed by metagenomic (green, MG) and metaproteomic (purple, MP) analysis. C) Violin-box plots showing the distribution of dissimilarity analysis of microbial community composition tested by pairwise Jaccard distances. P values: *** < 0.001, 0.001≤** <0.01. D) Taxonomic tree of biofilm microorganisms from domain to genus level. The entire taxonomic tree was constructed based on the biofilm metagenome, with bean green nodes representing members that also occur in the metaproteome. The size of the nodes indicates the* log*10 transformed relative abundances of microbes in the metagenome.*

For microbial community composition, both MP and MG revealed that the biofilm in shower hoses was dominated by bacteria, particularly Proteobacteria, which accounted for 99.9 ± 0.04 % (MP, total protein) and 99.7 ± 0.4 % (MG, total DNA). Eukaryota were ubiquitous and diverse (390/1459 genera) in the MG dataset(0.3 %), but not in the MP dataset (Fig. 2D). Archaea (0.002 %) and viruses (0.02 %) concentrations were low and only detected by MG. There were 110 shared genera identified by MP and MG, for which the vast majority were assigned as Alphaproteobacteria (82/110), Gamma- (9/110), and Beta-proteobacteria (7/110) (cladogram, Figure S2). Considering both MP and MG results, the most dominant *Hankyongella* spp. showed low expression level (MG: 20.5 ± 4.7 % vs. MP: 9.0 ± 3.4 %), while *Sphingomonas* spp. (MG: 4.7 ± 2.0 % vs. MP: 11.4 ± 6.7 %) and *Methylobacterium* spp. (MG: 2.7 ± 2.1 % vs. MP: 10.3 ± 3.3 %) showed high expression level. Regarding human (opportunistic) pathogens, among the 43 pathogen species indentified by MG, only 5 species were at sufficient levels that they could be detected by MP, indicating that gene-based studies can yield higher pathogen detection rates compared to proteomic approaches (Figure S3 and Table S5).

3.3. Global biofilm community functions

Overall, 45,516 genes (49.5 %) and 2659 proteins (69.9 %) were annotated using the KEGG database and assigned to 5644 and 1304 KOs, respectively. Pairwise Jaccard distances between MG and MP were similar to taxonomy-based analyses, suggesting that the expressed functions of biofilm microbiota differed significantly from their potential functions. The pairwise distances of taxa between samples were higher than those of function, revealing possible functional redundancy in shower hose microbial systems (Fig. 3A). Among all pathways, those related to metabolism functions were the most abundant (20.2–22.5 %) and exhibited even higher expression levels (22.5 %-30.3 %) (Fig. 3B). Particularly, the global and overview maps, amino acid metabolism, carbohydrate metabolism and energy metabolism were abundant and actively expressed (Fig. 3C). On the contrary, the expression levels of cellular processes and genetic information processing categories were low.

Biofilm formation genes. According to VFDB database, 188 genes involved in biofilm formation were extracted for in-depth analysis, among which 94 genes related to flagella, lateral flagella, and polar flagella were identified by MG and <1/3 of these genes were further detected by MP (29/94). The expressed genes include chemotaxis-

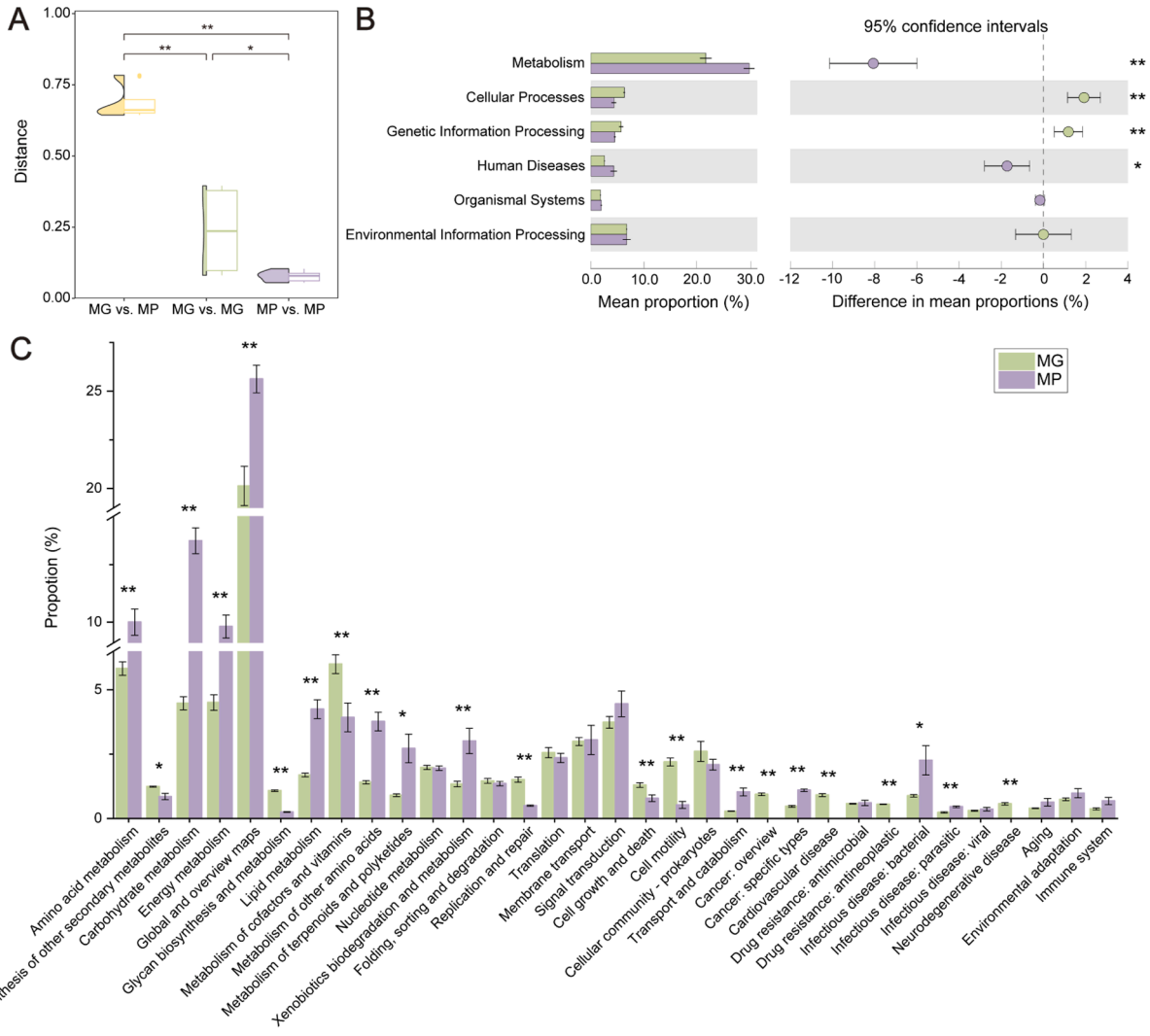

Fig. 3. Gene and protein function profiles based on KEGG database. *A) Violin-box plots showing the distribution of pairwise Jaccard distances of KO; B) Functional differences revealed by MG and MP at KEGG level 1; C) Relative abundances and significance analysis of functional categories at KEGG level 2. Asterisks indicate the statistically significant differences, P values: ** < 0.01, 0.01≤* <0.05.*

related genes (*cheA-Z*) that help cells sense chemical gradients and swim towards nutrients in the environment as well as fimbrial and non-fimbrial adhesins that are essential for the attachment of microbial cells to the surface (Fig. 4 and Table S6). Abundant non-fimbrial adhesin such as CadF and EF-Tu, were detected by both MG and MP, implying that non-fimbrial adhesin dominates the formation of environmental biofilms (Fig. 4B and C). Genes for extracellular structural proteins such as extracellular carbohydrate-binding proteins (lectin) and eDNA-binding proteins (DNABII family), were also present in high abundances with high expression levels. This is consistent with the visual characterization mentioned above. Most of other genes were not expressed regardless of their abundances detected by MG, such as bacterial amyloid fibers (e.g., cgsD genes), pili assembly genes (e.g., type IV pili), exopolysaccharides synthesis genes (e.g., alginate, cellulose, pel, psl), and genes for enzymes (diguanylate cyclases and phosphodiesterases) that participate in cyclic dimeric guanosine monophosphate turnover (Fig. 4B and C).

Disinfectant resistant genes. Disinfectant resistance is critical for microbial survival in drinking water systems, with glutathione (GSH) metabolism recognized as a key protective mechanism for biofilms against disinfectant residuals. In the KEGG GSH metabolism pathway, 24 out of the 39 enzymes were detected by MG, whereas only 13 were detected by MP. This suggests that the shower hose biofilm was enriched for (abundant) microbes that expressed genes for GSH synthesis and degradation. Based on the obtained MP results, a related pathway containing 29 enzymes was reconstructed in Fig. 5A. Two of the three known enzymes for glutathione synthesis were detected, i.e. glutathione reductase (GSH-R) and glutathione synthase (GSH-S). The latter should be the primary functional pathway in shower hose biofilm as it has much higher expression than GSH-R (Fig. 5B). For GSH degradation, multiple enzymes such as glutathione S-transferase (GST), gamma-glutamyl transpeptidase (GGT) and glutathione peroxidase (GPX), were detected. The content and expression level of GST (0.2 % and 1.1 %, catalyzing GSH and organic halides) were much higher than that of GPX (0.04 % and 0.005 %, catalyzing GSH and active oxides), indicating that the non-redox tolerance mode of biofilm microorganisms was stronger than the redox tolerance mode (Fig. 5B). Moreover, several genes of SoxRS, OxyR and RpoS systems were detected by both MG and MP, indicating that the shower hose biofilm responded to residual chlorine by activating multiple oxidation-resistant systems rather than relying on a single protective mechanism (Figure S4).

3.4. Effects of water heater temperatures

Generally, water heater temperature clearly affected the biomass, microbial communities and functional profiles of shower hose biofilms.

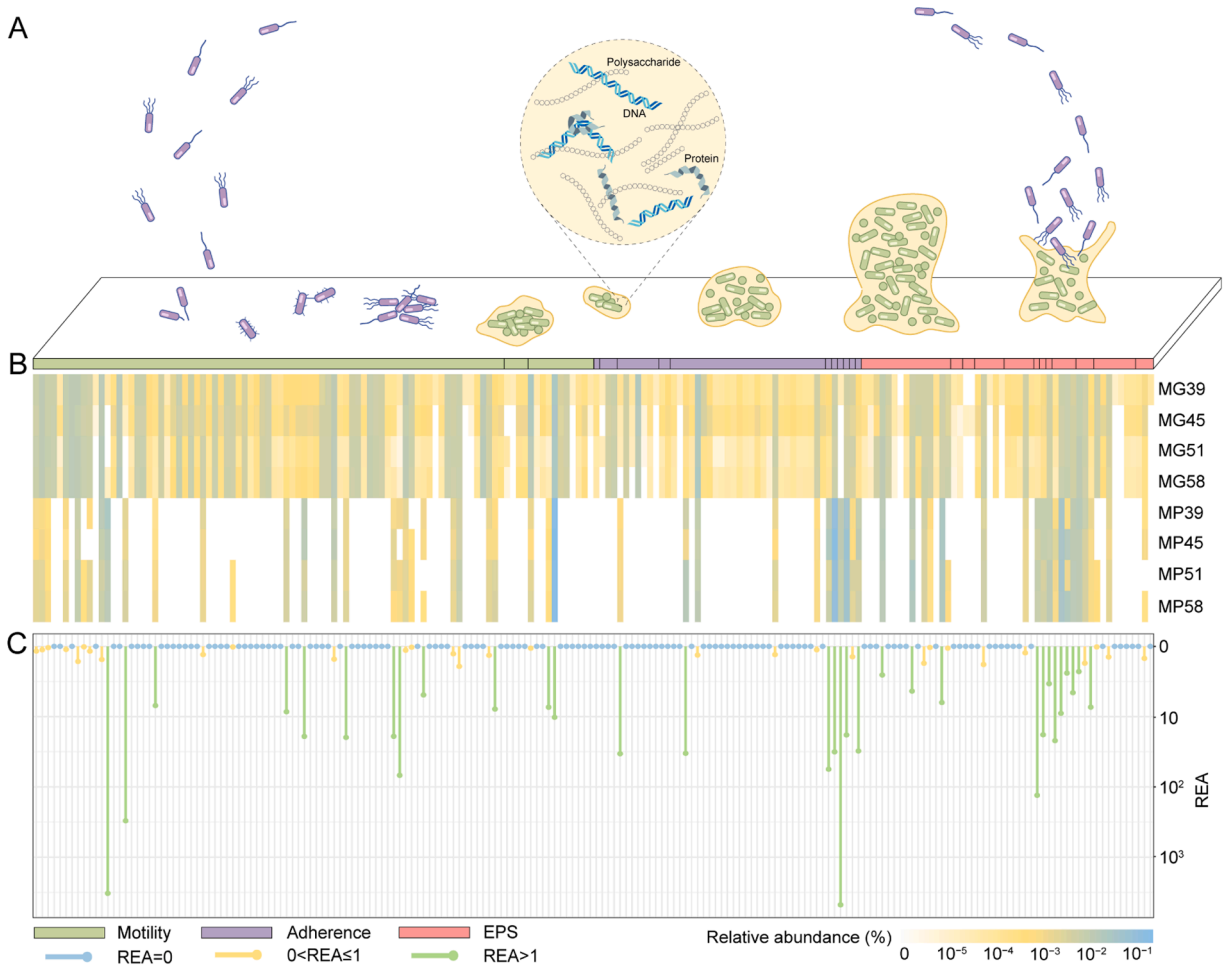

Fig. 4. Biofilm formation. *A) A classical conceptual model of biofilm formation and the major components and non-homogeneous distributed pattern of the extracellular polymeric substances' matrix. B)* Log*10 transformed relative abundances of genes and proteins involved in biofilm formation in different samples. The sub-categories of those genes from left to right are flagella, lateral flagella, polar flagella, curli fibers, flp pili, flp type IV pili, type 1 fimbriae, type IV pili, cadF, EF-Tu, etpA, hsp60, lap, PEB1, alginate, cellulose, Pel, Psl, VPS, bopD, bap, lectin, DNABII, adeFGH efflux pump, DGCs, PDEs. C)* Log*10 transformed relative expression activity of genes related to biofilm formation.*

As shown in Fig. 6A, the TCC values decreased linearly with the increase in water heater temperatures. Differently, the lowest ATP concentrations were achieved by setting instant heating temperature at 45 °C. When the instant heating temperature was at 39 °C, 51 °C and 58 °C, the ATP concentrations became two to three times higher than that at 45 °C, indicating 45 °C exhibited unique advantages in limiting active biomass.

According to MG and MP data, the number of identified genes (and therefore microbial diversity) decreased significantly with the increase in temperature, showing a sharp decline from 39 to 45 °C (86,371 to 48,008, 44.4 %), followed by smaller reductions at 51 °C (48,008 to 42,017, 7.0 %) and 58 °C (42,017 to 34,550, 8.6 %). In contrast, the number of proteins decreased more gradually with rising temperature, with only a slight reduction (88 proteins, 2.4 %) compared to the gene-level decline (Table S3). This was also expected, because the proteins represent the major microbes active in the community and a deeper coverage is often limited by the measurement effort and not by the complexity of the community. However, comparing the influence of temperature setting, there were 26,664 genes (29.0 %) and 2678 proteins (70.4 %) shared by four temperatures. It indicates that the genomic approach can overestimate temperature-induced influences because it more apparently influenced lower abundant microbes (Figure S5).

Considering both shared and unique genes and proteins between samples, as many as 32,279, 3297, 1369 and 137 unique genes were observed at temperatures of 39 °C, 45 °C, 51 °C and 58 °C, respectively, which decreased sharply with increasing heating temperature. Remarkably, no unique proteins were detected among the samples, indicating that the proteomic profiles showed less variation between biofilms compared to the genomic data. Taking 39 °C as baseline dataset, there were 71 proteins shared at 45 °C, 51 °C and 58 °C but not at 39 °C. When the temperature was set to 45 °C, 51 °C and 58 °C, 265, 522 and 427 proteins expressed at 39 °C disappeared, while 177, 186 and 240 proteins emerged, respectively (Figure S5).

At the genus level, the number of detected genera by MG decreased sharply from 1412 at 39 °C to 804 at 45 °C, and then gradually declined to 693 at 51 °C and 627 at 58 °C.. On the other hand, MP results showed rather a stable number of detected genera (89–102) (Table S4). Differences in the number of genera between samples could be attributed to the presence or absence of some low abundance microbes (<0.1 %). The dominant genera were the same across all four temperatures, but with varying relative abundances (Fig. 6B). Specifically, MG results showed that *Hankyongella* spp. (13.8 - 25.1 %) dominated all temperatures, with the lowest relative abundance detected at 45 °C and highest relative abundance at 51 °C (25.1 %) and 58 °C (24.8 %). According to MP results, 39 °C was dominated by *Hyphomicrobium* spp. (11.8 %), 45 °C was dominated by *Sphingomonas* spp. (22.7 %) and *Zymomonas* spp. (17.0 %), 51 °C was dominated by *Methylobacterium* spp. (15.9 %) and *Hankyongella* spp. (12.9 %) and 58 °C was dominated by *Hankyongella* spp. (11.6 %).

According to MG results, the number of (opportunistic) pathogens detected in biofilm samples decreased from 37 at 39 °C to 31 at 45 °C

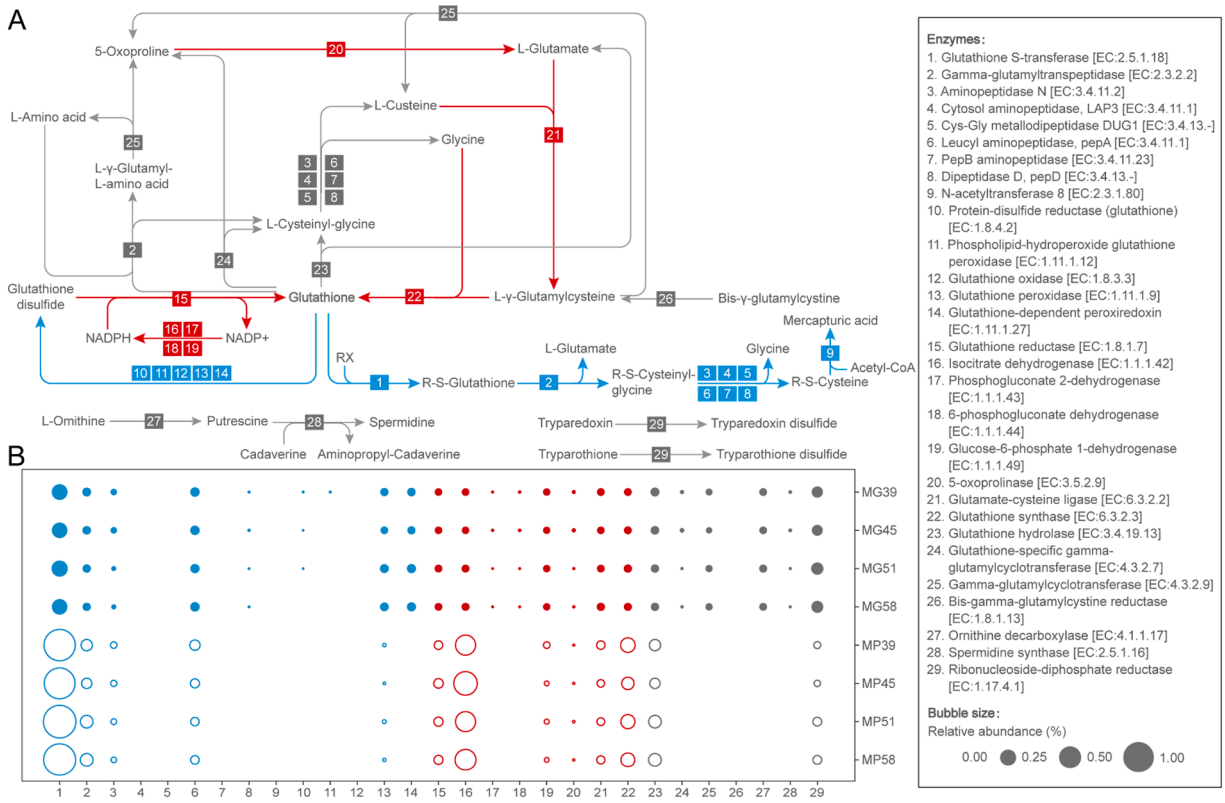

Fig. 5. Glutathione (GSH) metabolism pathway. *A) Reconstructed KEGG pathway for glutathione metabolism; B) Relative abundances of annotated enzymes associated with glutathione metabolism. Red = GSH synthesis related enzymes, blue = GSH degradation-related enzymes, grey = other enzymes.*

and further decreased declined to 22 at 51 °C and 26 at 58 °C (Figure S3). However, their relative abundances did not decrease, but increased from 0.1 % at 39 °C and 45 °C to 0.5 % at 51 °C and 58 °C. In the MP dataset, the number of detected pathogens significantly decreased, with only three to five species remaining, including *Sphingomonas paucimobilis, Salmonella enterica, Pseudomonas aeruginosa, Escherichia coli,* and *Klebsiella pneumoniae*. The total relative abundance of these species increased from 0.2 % at 39 °C to 0.4 % at 51 °C and 0.3 % at 58 °C. Remarkably, the lowest relative abundance of OPs was observed at 45 °C, accounting for only 0.03 % (Fig. 6C and S3). Notably, the enrichment and expression of genes and enzymes associated with disinfectant resistance and biofilm formation were virtually unaffected by water heater temperature, implying that different microbiomes have the same survival and biofilm formation mechanisms (Figs. 4B and 5B).

4. Discussion

4.1. Insights on shower biofilm from multi-omics profiles

In this study, significantly higher species richness and KOs richness were observed in the metagenomics data of shower hose biofilms compared to metaproteomics (Figs. 2A-C and 3A-C). As metaproteomics does not amplify before analysis, it mainly covers the dominant and active community. Moreover, the DNA-displayed total community includes not only active microorganisms but also dead and dormant microorganisms, as well as abundant eDNA that we observed (Fig. 1C and 1F). Previous studies reported that extracellular DNA accounts for an average of about 33 % of the total DNA pool in environmental samples, and even exceeding 80 % in some samples, which significantly affects the estimation of microbial community structure and diversity (Lennon et al., 2018). The sensitivity limitations of metaproteomics toward low abundance peptides also increased those discrepancies (Saito et al., 2019). However, the dominant genera of the total and active microbial communities were essentially the same, with most belonging to the Sphingomonadaceae family. The relative abundances of dominant genera in the latter were more evenly distributed (Fig. 6B and S2). The vast majority of MG detected pathogens (38/43) were not detected in the protein dataset. Only individual OPs (5/43) could be detected, implying that previous gene-based, in particular 16S rRNA gene sequencing-based studies perhaps overestimated the biological risk in drinking water systems (Feazel et al., 2009; Proctor et al., 2018; Rhoads et al., 2015; Ji et al., 2017; Proctor et al., 2017). Metaproteomic analyses can more accurately determine which OPs should be prioritized for surveillance, as they require active microbes at higher levels.

Combined metagenomic and metaproteomic analyses can also decipher biofilm formation and survival mechanisms. Flagella, non-fimbrial adhesins, alginate and extracellular structural proteins have been shown to play important roles in environmental biofilm formation. Compared to previous studies on freshwater and drinking water biofilms, this further expanded our understanding of key genes involved in natural biofilm formation (Breitbart et al., 2009; Chao et al., 2015). The low expression activity of flagellum-associated genes and c-di-GMP regulatory enzyme-related genes as well as the visualization results proved that the current biofilm is in a relatively stable state (Figs. 1 and 4B). According to previous DWDS biofilm studies, shower hose biofilm microbiome responded to the selective pressure of chlorination via multiple antioxidant systems (Chao et al., 2015). The results of multi-omics, especially metaproteomics, strongly suggest that the GST-mediated non-redox tolerance mode was the main detoxification pathway of the microbiota (Fig. 5). It indicated that most chlorinated and disinfected by-products in the cells were converted to xenobiotics substrates and then discharged to the environment (Margalef-Catala et al., 2017). The protective effect of GSH on microorganisms could explain the absolute dominance of Alphaproteobacteria in the communities, which usually contain GSH synthesizing genes and could be highly resistant to chlorination (Chao et al., 2015). Additionally,

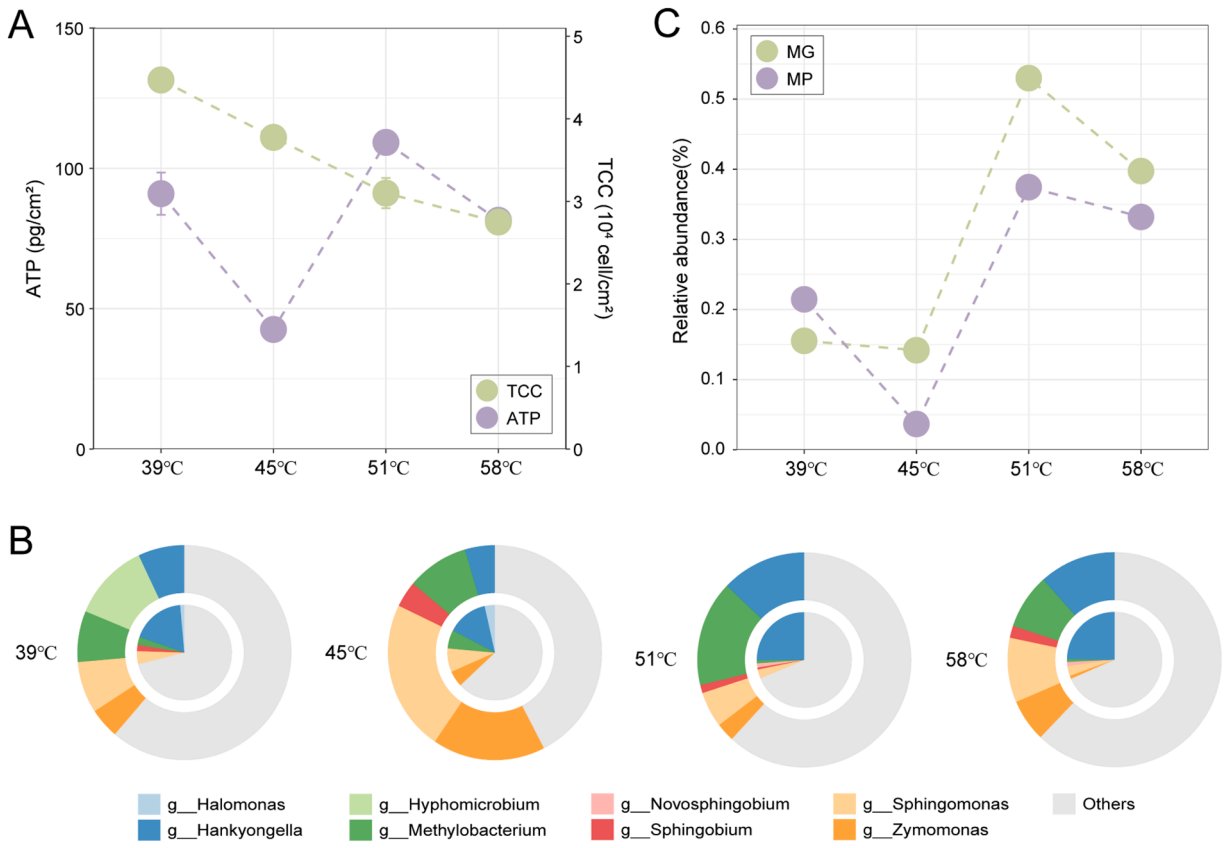

Fig. 6. The biofilms at different water heater temperatures. *A) Biomass of shower hoses biofilm measured by ATP (purple) and TCC (green). Data are presented as the means ± standard deviation, n = 3. B) The relative abundances of top5 genera in different metagenomic (inner ring) and metaproteomic (outer ring) samples. C) Total relative abundances of (opportunistic) pathogens in metagenomic (green) and metaproteomic (purple) samples.*

superoxide in biofilms is degraded by superoxide dismutase (sodA and sodC) to H_2O_2, and the latter is further decomposed by catalase (katE and katG). The TCA cycle genes acnA (aconitase A) and fumC (fumarase C) were highly activated by the SoxRS system, implying that the microbiota operated the TCA cycle to replenish NADPH/NADH pools depleted by detoxification, repair and protection processes to maintain redox balance (Sund et al., 2008).

4.2. *Instant heating to 45 °C may be the golden solution for showering*

As shown in this study, 45 °C temperature setting could represent an optimal balance, as it not only minimizes active biomass (measured by ATP) but also shows lowest number and relative abundance of pathogens (determined through multi-omics analysis) (Fig. 6A and C). This challenges previous notions that raising water heater temperatures would inhibit the growth of OPs (Darelid et al., 2002bib59; World Health Organization 2024, National Academies of Sciences E, Medicine 2020, Centers for Disease Control and Prevention 2024). This may be due to our novel investigation of shower hose biofilm exposed to typical showering water at 39 °C, regardless of the heating temperature. Our findings highlight that temperature control, which does not extend to the point of use, is insufficient to manage biological risks. Higher heating temperatures result in the introduction of more cold water before it flows through the shower hoses. This influx of cold water may facilitate the colonization of OPs due to the direct diffusion of cold water at a favorable temperature (Proctor et al., 2018, Rhoads et al., 2015, Proctor et al., 2017). For instance, we observed an increase in the total relative abundances of OPs in systems heated to 51 °C and 58 °C, attributed to the proliferation of *Sphingomonas paucimobilis*. Since this species typically does not thrive above 42 °C, it is likely introduced through the direct mixing of cold water (Morrison and Shulman, 1986).

This study utilized instant water heaters instead of storage water heaters, thereby eliminating the prolonged storage of heated water and the associated high risk of opportunistic pathogens (OPs) growth. Prior research has indicated that the risk of *Legionella* in plumbing systems equipped with instant water heaters is significantly lower compared to those with storage water heaters (Martinelli et al., 2000, Mathys et al., 2008). Apart from the reduced risk of OPs, on-demand instant systems operate with nearly 100 % energy efficiency and consume 8–50 % less energy than storage heater systems (Brazeau and Edwards, 2011, Brazeau and Edwards, 2013). Therefore, based on the findings of this study, instant heating to 45 °C may represent the optimal showering solution while effectively balancing physical safety, biosafety and energy conservation.

4.3. *Implications and outlook*

This study employed metagenomics and metaproteomics to investigate microbial diversity, genetic potential and protein expression in shower hose biofilms under varying heating temperatures. This integrative approach provided insights into the dynamic responses and functional mechanisms of the bacterial communities, which are crucial for both scientific understanding and for finding practical solutions. For instance, we found that relying solely on gene-based analysis could overestimate pathogen risks in shower biofilms and potentially lead to misleading management strategies, as different pathogens may require distinct treatments. A combination like this could also be applied to studying other water-related biological processes and issues such as biofouling in membrane and sand filtration systems, biocorrosion of metal materials and pipes as well as the sudden release of biofilm during transitions in drinking water systems due to changes in water source or

quality.

As mentioned earlier, determining the optimal heating temperature for showering involves striking a delicate balance between ensuring public health and reducing energy consumption (Shen et al., 2022, Krovel et al., 2022, Brazeau and Edwards, 2011, Brazeau and Edwards, 2013). The identification of 45 °C as an optimal solution at the last meter of shower system suggests the existence of a possible threshold temperature that reconciles these goals. However, the exact optimal temperature may vary depending on the water quality of different systems. For instance, our previous research indicated that extremely low levels of assimilable organic carbon (AOC, <1 μg/L) can effectively limit the growth of opportunistic pathogens like *Legionella*, potentially obviating the need for high temperatures to ensure biosafety (Learbuch et al., 2019). Moreover, there may be other temperature settings between 39 °C and 45 °C that could achieve even lower temperatures while still maintaining biosafety. Further research is needed to explore the possible relationships between temperature settings and water quality parameters, particularly AOC levels.

It's important to note that this study was conducted in full-scale shower systems, which allowed us to isolate other factors and systematically investigate the effects of water heater temperature on biofilm communities and biosafety. However, given the complexity of real-life situations, such as the cross-influence of showering frequency and plumbing materials, studies targeting actual shower hose biofilms are necessary. Furthermore, this study provided only a snapshot sampling and thus, dynamic as well as long-term succession should be investigated to gain a more comprehensive understanding of microbial communities in shower hose biofilms.

CRediT authorship contribution statement

Mingchen Yao: Writing – original draft, Investigation, Conceptualization. **Anran Ren:** Writing – original draft, Visualization, Investigation, Formal analysis, Conceptualization. **Xiangyu Yang:** Writing – review & editing. **Lihua Chen:** Writing – review & editing. **Xun Wang:** Writing – review & editing. **Walter van der Meer:** Writing – review & editing. **Mark C.M. van Loosdrecht:** Writing – review & editing. **Gang Liu:** Writing – review & editing, Funding acquisition, Conceptualization. **Martin Pabst:** Writing – review & editing, Conceptualization.

Declaration of competing interest

The authors declare that they have no known competing financial interests or personal relationships that could have appeared to influence the work reported in this paper.

Acknowledgments

The present work has been financially supported by the National Natural Science Foundation of China (Basic Science Center Project, 52388101; 52370105; 52022103).

Supplementary materials

Supplementary material associated with this article can be found, in the online version, at doi:10.1016/j.watres.2024.122704.

Data availability

Data will be made available on request.

References

Allaire, J, 2012. RStudio: integrated development environment for R. Boston, MA 770 (394), 165–171.

Brazeau, RH, Edwards, MA., 2011. A Review of the Sustainability of Residential Hot Water infrastructure: Public health, Environmental impacts, and Consumer Drivers, 6. College Publishing, pp. 77–95.

Brazeau, RH, Edwards, MA., 2013. Water and energy savings from on-demand and hot water recirculating systems. J. Green Build. 8 (1), 75–89.

Breitbart, M, Hoare, A, Nitti, A, Siefert, J, Haynes, M, Dinsdale, E, et al., 2009. Metagenomic and stable isotopic analyses of modern freshwater microbialites in Cuatro Cienegas. Mexico. Environ Microbiol. 11 (1), 16–34. https://doi.org/10.1111/j.1462-2920.2008.01725.x.

Bucheli-Witschel, M, Kotzsch, S, Darr, S, Widler, R, Egli, T., 2012. A new method to assess the influence of migration from polymeric materials on the biostability of drinking water. Water Res. 46 (13), 4246–4260. https://doi.org/10.1016/j.watres.2012.05.008.

Buchfink, B, Xie, C, Huson, DH., 2015. Fast and sensitive protein alignment using DIAMOND. Nat. Methods 12 (1), 59–60. https://doi.org/10.1038/nmeth.3176.

Buzzo, JR, Devaraj, A, Gloag, ES, Jurcisek, JA, Robledo-Avila, F, Kesler, T, et al., 2021. Z-form extracellular DNA is a structural component of the bacterial biofilm matrix. Cell 184 (23). https://doi.org/10.1016/j.cell.2021.10.010, 5740-58 e17.

Cavallaro, A, Rhoads, WJ, Sylvestre, É, Marti, T, Walser, J-C, Hammes, F., 2023. Legionella relative abundance in shower hose biofilms is associated with specific microbiome members. Biorxiv. https://doi.org/10.1101/2023.05.04.539404, 2023.05.04.539404.

Centers for Disease Control and Prevention. Controlling Legionella in Potable Water Systems. https://www.cdc.gov/legionella/wmp/control-toolkit/potable-water-systems.html Accessed 2024.

Chao, Y, Mao, Y, Wang, Z, Zhang, T, 2015. Diversity and functions of bacterial community in drinking water biofilms revealed by high-throughput sequencing. Sci. Rep. 5, 10044. https://doi.org/10.1038/srep10044.

Chen, MY, Lee, DJ, Tay, JH, Show, KY., 2007. Staining of extracellular polymeric substances and cells in bioaggregates. Appl. Microbiol. Biotechnol. 75 (2), 467–474. https://doi.org/10.1007/s00253-006-0816-5.

Chen, S, Zhou, Y, Chen, Y, Gu, J., 2018. fastp: an ultra-fast all-in-one FASTQ preprocessor. Bioinformatics 34 (17), i884–ii90. https://doi.org/10.1093/bioinformatics/bty560.

Collier, SA, Deng, L, Adam, EA, Benedict, KM, Beshearse, EM, Blackstock, AJ, et al., 2021. Estimate of burden and direct healthcare cost of infectious waterborne disease in the United States. Emerging Infect. Dis. 27 (1), 140.

Cox, J, Mann, M., 2008. MaxQuant enables high peptide identification rates, individualized p.p.b.-range mass accuracies and proteome-wide protein quantification. Nat. Biotechnol. 26 (12), 1367–1372. https://doi.org/10.1038/nbt.1511.

Dai, Z, Sevillano-Rivera, MC, ST, Calus, Bautista-de Los Santos, QM, Eren, AM, van der Wielen, P, et al., 2020. Disinfection exhibits systematic impacts on the drinking water microbiome. Microbiome 8 (1), 42. https://doi.org/10.1186/s40168-020-00813-0.

Darelid, J, Lofgren, S, Malmvall, BE., 2002. Control of nosocomial Legionnaires' disease by keeping the circulating hot water temperature above 55 °C: experience from a 10-year surveillance programme in a district general hospital. J. Hosp. Infect. 50 (3), 213–219. https://doi.org/10.1053/jhin.2002.1185.

Edition, F., 2011. Guidelines for drinking-water quality. WHO Chron. 38 (4), 104–108.

Falkinham, J, Pruden, A, Edwards, M., 2015. Opportunistic premise plumbing pathogens: increasingly important pathogens in drinking water. Pathogens. 4 (2), 373–386. https://doi.org/10.3390/pathogens4020373.

Feazel, LM, Baumgartner, LK, Peterson, KL, Frank, DN, Harris, JK, Pace, NR., 2009. Opportunistic pathogens enriched in showerhead biofilms. Proc. Natl. Acad. Sci. 106 (38), 16393–16399. https://doi.org/10.1073/pnas.0908446106.

Fu, L, Niu, B, Zhu, Z, Wu, S, Li, W., 2012. CD-HIT: accelerated for clustering the next-generation sequencing data. Bioinformatics 28 (23), 3150–3152. https://doi.org/10.1093/bioinformatics/bts565.

Gebert, MJ, Delgado-Baquerizo, M, Oliverio, AM, Webster, TM, Nichols, LM, Honda, JR, et al., 2018. Ecological analyses of mycobacteria in showerhead biofilms and their relevance to human health. mBio 9 (5). https://doi.org/10.1128/mBio.01614-18.

Hammes, F, Berney, M, Wang, Y, Vital, M, Koster, O, Egli, T., 2008. Flow-cytometric total bacterial cell counts as a descriptive microbiological parameter for drinking water treatment processes. Water Res. 42 (1–2), 269–277. https://doi.org/10.1016/j.watres.2007.07.009.

Hyatt, D, Chen, GL, Locascio, PF, Land, ML, Larimer, FW, Hauser, LJ., 2010. Prodigal: prokaryotic gene recognition and translation initiation site identification. BMC Bioinf. 11, 119. https://doi.org/10.1186/1471-2105-11-119.

Ji, P, Rhoads, WJ, Edwards, MA, Pruden, A., 2017. Impact of water heater temperature setting and water use frequency on the building plumbing microbiome. ISME J. 11 (6), 1318–1330. https://doi.org/10.1038/ismej.2017.14.

Kanehisa, M, Sato, Y, Kawashima, M, Furumichi, M, Tanabe, M., 2016. KEGG as a reference resource for gene and protein annotation. Nucleic. Acids. Res. 44 (D1), D457–D462. https://doi.org/10.1093/nar/gkv1070.

Kassambara, A., 2019. rstatix: pipe-friendly framework for basic statistical tests. CRAN: Contributed Packages.

Keiblinger, KM, Wilhartitz, IC, Schneider, T, Roschitzki, B, Schmid, E, Eberl, L, et al., 2012. Soil metaproteomics - Comparative evaluation of protein extraction protocols. Soil Biol. Biochem. 54 (15–10), 14–24. https://doi.org/10.1016/j.soilbio.2012.05.014.

Kleikamp, HBC, Grouzdev, D, Schaasberg, P, van Valderen, R, van der Zwaan, R, Wijgaart, RV, et al., 2023. Metaproteomics, metagenomics and 16S rRNA sequencing provide different perspectives on the aerobic granular sludge microbiome. Water Res. 246, 120700. https://doi.org/10.1016/j.watres.2023.120700.

Krovel, AV, Bernhoff, E, Austerheim, E, Soma, MA, Romstad, MR, Lohr, IH., 2022. Legionella pneumophila in Municipal Shower Systems in Stavanger, Norway; A longitudinal surveillance study using whole genome sequencing in risk management. Microorganisms 10 (3). https://doi.org/10.3390/microorganisms10030536.

Learbuch, KLG, Lut, MC, Liu, G, Smidt, H, van der Wielen, P., 2019. Legionella growth potential of drinking water produced by a reverse osmosis pilot plant. Water Res. 157, 55–63. https://doi.org/10.1016/j.watres.2019.03.037.

Lennon, J, Muscarella, M, Placella, S, Lehmkuhl, B., 2018. How, when, and where relic DNA affects microbial diversity. mBio 9 (3) e00637-18.

Li, D, Liu, CM, Luo, R, Sadakane, K, Lam, TW., 2015. MEGAHIT: an ultra-fast single-node solution for large and complex metagenomics assembly via succinct de Bruijn graph. Bioinformatics 31 (10), 1674–1676. https://doi.org/10.1093/bioinformatics/btv033.

Li, R, Li, Y, Kristiansen, K, Wang, J., 2008. SOAP: short oligonucleotide alignment program. Bioinformatics 24 (5), 713–714. https://doi.org/10.1093/bioinformatics/btn025.

Liu, B, Zheng, D, Zhou, S, Chen, L, Yang, J., 2022. VFDB 2022: a general classification scheme for bacterial virulence factors. Nucleic. Acids. Res. 50 (D1), D912–D9D7. https://doi.org/10.1093/nar/gkab1107.

Luber, CA, Cox, J, Lauterbach, H, Fancke, B, Selbach, M, Tschopp, J, et al., 2010. Quantitative proteomics reveals subset-specific viral recognition in dendritic cells. Immunity 32 (2), 279–289. https://doi.org/10.1016/j.immuni.2010.01.013.

Margalef-Catala, M, Araque, I, Bordons, A, Reguant, C, 2017. Genetic and transcriptional study of glutathione metabolism in Oenococcus oeni. Int. J. Food Microbiol. 242, 61–69. https://doi.org/10.1016/j.ijfoodmicro.2016.11.013.

Martinelli, F, Caruso, A, Moschini, L, Turano, A, Scarcella, C, Speziani, F., 2000. A comparison of Legionella pneumophila occurrence in hot water tanks and instantaneous devices in domestic, nosocomial, and community environments. Curr. Microbiol. 41 (5), 374–376. https://doi.org/10.1007/s002840010152.

Mathys, W, Stanke, J, Harmuth, M, Junge-Mathys, E., 2008. Occurrence of Legionella in hot water systems of single-family residences in suburbs of two German cities with special reference to solar and district heating. Int. J. Hyg. Environ. Health 211 (1–2), 179–185. https://doi.org/10.1016/j.ijheh.2007.02.004.

McMurdie, PJ, Holmes, S., 2013. phyloseq: an R package for reproducible interactive analysis and graphics of microbiome census data. PLoS One 8 (4), e61217. https://doi.org/10.1371/journal.pone.0061217.

Morrison Jr, A, Shulman, J, 1986. Community-acquired bloodstream infection caused by Pseudomonas paucimobilis: case report and review of the literature. J. Clin. Microbiol. 24 (5), 853–855.

National Academies of Sciences E, Medicine, 2020. Management of Legionella in Water Systems. National Academies Press.

Proctor, CR, Dai, D, Edwards, MA, Pruden, A., 2017. Interactive effects of temperature, organic carbon, and pipe material on microbiota composition and Legionella pneumophila in hot water plumbing systems. Microbiome 5 (1), 130. https://doi.org/10.1186/s40168-017-0348-5.

Proctor, CR, Gächter, M, Kötzsch, S, Rölli, F, Sigrist, R, Walser, J-C, et al., 2016. Biofilms in shower hoses – choice of pipe material influences bacterial growth and communities. Environ. Sci.: Water Res. Technol. 2 (4), 670–682. https://doi.org/10.1039/c6ew00016a.

Proctor, CR, Reimann, M, Vriens, B, Hammes, F., 2018. Biofilms in shower hoses. Water Res. 131, 274–286. https://doi.org/10.1016/j.watres.2017.12.027.

R Core Team, 2013. R: A language and environment for statistical computing. Foundation for Statistical Computing, Vienna, Austria.

Ramírez-Castillo, F, Loera-Muro, A, Jacques, M, Garneau, P, Avelar-González, F, Harel, J, et al., 2015. Waterborne Pathogens: detection Methods and Challenges. Pathogens. 4 (2), 307–334. https://doi.org/10.3390/pathogens4020307.

Rhoads, WJ, Ji, P, Pruden, A, Edwards, MA, 2015. Water heater temperature set point and water use patterns influence Legionella pneumophila and associated microorganisms at the tap. Microbiome 3, 67. https://doi.org/10.1186/s40168-015-0134-1.

Rhoads, WJ, Pruden, A, Edwards, MA., 2016. Convective Mixing in Distal Pipes Exacerbates Legionella pneumophila Growth in Hot Water Plumbing. Pathogens 5 (1). https://doi.org/10.3390/pathogens5010029.

Saito, MA, Bertrand, EM, Duffy, ME, Gaylord, DA, Held, NA, WJt, Hervey, et al., 2019. Progress and challenges in ocean metaproteomics and proposed best practices for data sharing. J. Proteome Res. 18 (4), 1461–1476. https://doi.org/10.1021/acs.jproteome.8b00761.

Schoen, ME, Ashbolt, NJ., 2011. An in-premise model for Legionella exposure during showering events. Water Res. 45 (18), 5826–5836. https://doi.org/10.1016/j.watres.2011.08.031.

Shen, Y, Haig, SJ, Prussin 2nd, AJ, LiPuma, JJ, Marr, LC, Raskin, L., 2022. Shower water contributes viable nontuberculous mycobacteria to indoor air. PNAS Nexus 1 (5), pgac145. https://doi.org/10.1093/pnasnexus/pgac145.

Soto-Giron, MJ, Rodriguez, RL, Luo, C, Elk, M, Ryu, H, Hoelle, J, et al., 2016. Biofilms on hospital shower hoses: characterization and implications for nosocomial infections. Appl. Environ. Microb. 82 (9), 2872–2883. https://doi.org/10.1128/AEM.03529-15.

Sousi, M, Liu, G, Salinas-Rodriguez, SG, Knezev, A, Blankert, B, Schippers, JC, et al., 2018. Further developing the bacterial growth potential method for ultra-pure drinking water produced by remineralization of reverse osmosis permeate. Water Res. 145, 687–696. https://doi.org/10.1016/j.watres.2018.09.002.

Sund, CJ, Rocha, ER, Tzianabos, AO, Wells, WG, Gee, JM, Reott, MA, et al., 2008. The Bacteroides fragilis transcriptome response to oxygen and H2O2: the role of OxyR and its effect on survival and virulence. Mol. Microbiol. 67 (1), 129–142. https://doi.org/10.1111/j.1365-2958.2007.06031.x.

Tian, L, Wang, L., 2021. Multi-omics analysis reveals structure and function of biofilm microbial communities in a pre-denitrification biofilter. Sci. Total Environ. 757, 143908. https://doi.org/10.1016/j.scitotenv.2020.143908.

U.S. Department of Energy. Savings Project: Lower Water Heating Temperature. https://www.energy.gov/energysaver/do-it-yourself-savings-project-lower-water-heating-temperature Accessed 2024.

Wiśniewski, JR, Ostasiewicz, P, Duś, K, Zielińska, DF, Gnad, F, Mann, M., 2012. Extensive quantitative remodeling of the proteome between normal colon tissue and adenocarcinoma. Mol. Syst. Biol. 8 (1). https://doi.org/10.1038/msb.2012.44.

Woolhouse, M, Gowtage-Sequeria, S, Evans, B., 2007. T16: quantitative analysis of the characteristics of emerging and re-emerging human pathogens. The UK Government's Foresight Project Infectious Diseases: Preparing for the Future.

World Health Organization. Regional Office for E. Legionellosis. https://www.who.int/news-room/fact-sheets/detail/legionellosis Accessed 2024.

World Health Organization. Drinking-water. https://www.who.int/news-room/fact-sheets/detail/drinking-water Accessed 2024.

Yang, X, He, Q, Liu, T, Zheng, F, Mei, H, Chen, M, et al., 2022. Impact of microplastics on the treatment performance of constructed wetlands: based on substrate characteristics and microbial activities. Water Res. 217, 118430. https://doi.org/10.1016/j.watres.2022.118430.

Yao, M, Zhang, Y, Dai, Z, Ren, A, Fang, J, Li, X, et al., 2023. Building water quality deterioration during water supply restoration after interruption: influences of premise plumbing configuration. Water Res. 241, 120149. https://doi.org/10.1016/j.watres.2023.120149.